JCEC
THE JOURNAL OF ENGINEERING AND EXACT SCIENCES

OPEN ACCESS

The Journal of Engineering and Exact Sciences – jCEC, Vol. 10 N. 05 (2024)
journal homepage: https://periodicos.ufv.br/jcec
eISSN: 2527-1075
ISSN: 2446-9416

Sandwich structures with TPMS core and printed circuit board faces

Estruturas sanduíche com núcleo de TPMS e faces de placa de circuito impresso

Article Info:
Article history: Received 2024-02-02 / Accepted 2024-06-20 / Available online 2024-06-28
doi: 10.18540/jcecvl10iss5pp18973

Gustavo Ferreira Malta
ORCID: https://orcid.org/0009-0008-1610-3908
Universidade de Brasília, Brazil
E-mail: gustavof.malta10@gmail.com
Pedro Henrique dos Santos Alves
ORCID: https://orcid.org/0000-0002-1186-5750
Universidade de Brasília, Brazil
E-mail: pedrohenriquedf11@gmail.com
Manuel Nascimento Dias Barcelos Jr
ORCID: https://orcid.org/0000-0001-8795-8999
Universidade de Brasília, Brazil
E-mail: manuelbarcelos@unb.br

Abstract
Sandwich structures are widely used in the aerospace industries due to their mechanical properties that give them high energy absorption, low density, and high mechanical strength. These structures are composed of two faces interspersed by a core that can have various geometric configurations. One of the most widely used geometric cells are honeycomb structures, highly used in structural applications since the early 20th century. However, new geometric core configurations, as well as alternative materials and manufacturing processes, are being studied for space applications. Triply Periodic Minimal Surfaces (TPMS) are lattice structures composed of periodic surface structures in three independent directions. Among the available models, the most notable TPMS structures are Schwartz-type, Diamond-type, and Gyroid-type. Since the structures are too complex to be manufactured by subtractive manufacturing, additive manufacturing is excellent, being able to produce complex structures much faster and easier. One of the most common types of 3D printing is Fused Deposition Modeling (FDM), which is based on the fusion and deposition of various materials, such as thermoplastic materials. To save space and improve the mechanical strength of Cubesats, sandwich structures are being produced using printed circuit boards (PCB) of electrical and electronic components as outer faces. These faces are called laminates and are made of thermosetting materials such as fiberglass and epoxy resin, composites, or ceramic materials. The objective of this paper is to produce sandwich panels, with a core based on the TPMS architecture. They will be printed in thermoplastic material with laminated faces used in printed circuit boards. A numerical analysis using the finite element method was performed and its testing according to ASTM C393, furthermore, this paper aims to realize an optimized TPMS core with mass distribution based on the stress profile and compare them.
Keywords: Sandwich Structures. Topology Optimization. TPMS. 3D printing. Finite Element Method.

Resumo
As estruturas sanduíche são amplamente utilizadas nas indústrias aeroespaciais devido às suas propriedades mecânicas que lhes conferem alta absorção de energia, baixa densidade e alta resistência mecânica. Essas estruturas são compostas por duas faces intercaladas por um núcleo que

pode ter várias configurações geométricas. Uma das células geométricas mais amplamente utilizadas são as estruturas de favo de mel, altamente utilizadas em aplicações estruturais desde o início do século XX. No entanto, novas configurações geométricas de núcleo, assim como materiais e processos de fabricação alternativos, estão sendo estudados para aplicações espaciais. As Superfícies Mínimas Triplamente Periódicas (TPMS) são estruturas de grade compostas por estruturas de superfície periódicas em três direções independentes. Entre os modelos disponíveis, as estruturas TPMS mais notáveis são do tipo Schwartz, do tipo Diamante e do tipo Giroide. Como as estruturas são muito complexas para serem fabricadas por manufatura subtrativa, a manufatura aditiva é excelente, sendo capaz de produzir estruturas complexas muito mais rapidamente e facilmente. Um dos tipos mais comuns de impressão 3D é a Modelagem por Fusão e Deposição (FDM), que é baseada na fusão e deposição de vários materiais, como materiais termoplásticos. Para economizar espaço e melhorar a resistência mecânica dos Cubesats, estruturas sanduíche estão sendo produzidas usando placas de circuito impresso (PCI) de componentes elétricos e eletrônicos como faces externas. Essas faces são chamadas de laminados e são feitas de materiais termofixos como fibra de vidro e resina epóxi, compósitos ou materiais cerâmicos. O objetivo deste trabalho é produzir painéis sanduíche, com um núcleo baseado na arquitetura TPMS. Eles serão impressos em material termoplástico com faces laminadas usadas em placas de circuito impresso. Foi realizada uma análise numérica usando o método dos elementos finitos e seu teste de acordo com ASTM C393, além disso, este trabalho visa realizar um núcleo TPMS otimizado com distribuição de massa com base no perfil de estresse e compará-los.
Palavras-chave: Estruturas Sanduíche. Otimização Topológica. Superfícies Mínimas Triplamente Periódicas (TPMS). Impressão 3D. Método dos Elementos Finitos.

1. Introduction

The Triply Periodic Minimal Surfaces (TPMS) were described by Schwarz in 1865 (Han and Che, 2018). These structures are periodic in the three principal directions and are also non-self-intersecting. The first geometries discovered were named as Primitive (or Shwarz), Diamond, Hexagonal and Neoviuos. However, the most popular geometry, the Gyroid, was only discovered in 1970 by Schoen (Hermann and Konrad, 1996).

Nowadays, it is possible to manufacture complex geometries like TPMS thanks to advances in Additive Manufacturing (Hsieh and Valdevit, 2020). This technology allows the production of parts and prototypes using computer-aided design (CAD) softwares, thus reducing the steps required to obtain a final product (Gibson *et al.*, 2015). Once the 3D model is ready, it is possible to produce the provided model using 3D printing. The most common and cost-effective 3D printing manufacturing method is the Fused Deposition Modelling (FDM) (Vyavahare *et al.*, 2020). This manufacturing method is highly used in the aerospace, automotive and biotechnology industries due to its high added benefits (Zou *et al.*, 2016). A Printed Circuit Board (PCB) is a platform where it is possible to place microelectronic components and is widely found in basically all electronic products (LaDou, 2006). PCBs have two main parts, a base, which is also called laminate, which is composed of dielectric material, and the second part, a thin copper layer where the circuit is printed. The most common type of laminate is FR-4, a material made of fiberglass and epoxy resin, by which FR stands for flame retardant (Henrique Júnior *et al.*, 2013).

Optimization of structures can be classified into three categories: size optimization, geometrical optimization, and topological optimization. Topological optimization aims to find an optimal pattern that alternates solids and voids. This method is usually used at the conceptual stage to optimize properties such as stiffness and natural frequency of a structure (Zhang *et al.*, 2016). The implementation of optimization tools is highly important in most engineering fields, especially aerospace and aeronautics, lowering the costs of a structure and maintaining its integrity (Zhu *et al*., 2016).

The objective of this work is to carry out the production of sandwich panels, with the cores based on the TPMS architecture, printed on thermoplastic materials and with faces of laminated materials that are used in printed circuit boards, performing the numerical analysis by the finite

element method, and also performing the experimental characterization according to the ASTM C393 standard. In addition, this project also aims to perform a topological optimization of the TPMS core, with a mass distribution based on the internal forces and perform a comparison between the panels produced.

2. Theoretical background

A triply periodic surface is described as a mathematical surface in R^3 with minimum area and the average curvature equal to zero. The surfaces with minimum area have been studied for more than 200 years, through the studies of Lagrange (Decker and Frantz, 2022). The first TPMS was described as Scharz P, or the primitive. This geometry can be seen in Figure 1a. The equation that represents the TPMS Primitive is described in Eq. 1.

Figure 1 - Geometry Configurations. (a) TPMS Primitive (b) TPMS Diamond (c) TPMS Gyroid

Alongside with the Primitive, the geometry of Schwarz D or Diamond was also described. This configuration was known as Diamond because it resembles the chemical structure of the carbon atoms that forms the diamond. The TPMS Diamond is shown in Figure 1b. The Eq. 2 is used to describe the geometry.

A couple of years later, in 1970, Alan Schoen described a new structure, the gyroid. For example, the gyroid can be found in nature in the wings of butterflies. The TPMS Gyroid can be seen in Figure1c. This structure is described by the Eq. 3.

$$\cos x + \cos y + \cos z = 0 \quad (1)$$

$$\sin x \sin y \sin z + \sin x \cos y \cos z + \cos x \sin y \cos z + \cos x \cos y \sin z = 0 \quad (2)$$

$$\sin x \cos y + \sin y \cos z + \sin z \cos x \quad (3)$$

3.Sandwich Structures

Sandwich Structures are usually made from 2 faces of a resistant material on its exterior and a core of another material. The sandwich structures, in general, are used due to its properties of bending resistance, energy absorption and acoustic and thermal isolation (Gagliardo and Mascia, 2010).

The core that separates the 2 faces increases the moment of inertia, increasing its resistance to flexion Bitzer (1997). The most used core in sandwich panels is honeycomb. However, studies using porous cores have been intensified, mainly due to the possibility of performing the topological optimization of the structures. (Tran and Peng, 2021)

The application for this type of structure is widely varied due to its versatility, therefore, they can be found in commercial aviation considering the need to lower the mass of the airplane and maintaining its mechanical resistance (Shwingel *et al.*, 2007). Other applications for sandwich structures are space vehicles that have the same necessity of a light and strong structure as aeronautics vehicles but also good thermal properties, such as Cubesats that need to maintain a low mass budget.

4. Finite Element Method

The Finite Element Method (FEM) is a numeric procedure used to obtain solutions for engineering problems that may or may not be resolved in an analytic way. It was first originated by Courant, who, in his article, utilized polynomial interpolation to investigate torsion problems in a

triangular domain (Moaveni, 2007). Nowadays, any finite element analysis can be divided into 7 steps.

The first step is to create the mesh and perform the discretization, in other words, to divide the body in several elements, associated with nodes. The second step is to consider a function that represents the physical behavior of each element. Then, it is necessary to develop the equations for each element. The following steps are to build a global stiffness matrix and to apply the boundary conditions. Hence, it will be possible to solve the system and finally obtain relevant results.

The final objective of the analysis is to obtain relevant data and review it. Determining the critical points where the structure suffers big deformations or high concentration of stresses is an important step of the analysis (Logan, 2011).

This method is used for different areas of engineering calculations, principally mechanical applications, such as the ones used for this work. It's possible to encounter different commercial software capable of calculating mechanical properties using the Finite Element Method, such as Ansys Workbench.

5. Methods

5.1 Core modeling

To perform the study, destructive tests, according to the ASTM C393, were used to assess the mechanical properties of the sandwich panels manufactured. Furthermore, numeric analysis was made in order to validate the experimental properties.

The specimens were modeled with the assistance of the 3D modeling software, 3D nTopology. The core was initially modeled as a block of 200mm length, 75mm width and 16mm height. This size was defined by the standard ASTM C393. Afterwards, a TPMS cell was applied to the block, and an analysis was done following 3 patterns of cell: Primitive, Diamond and Gyroid.

For the Primitive's core, a 15mm edge was used. A 0.9 mm filling was applied. The core can be seen in Figure 2a. For the Diamond's core, a 15mm edge was also used. For this type of core, a 1.3mm filling was used. The core generated can be seen in Figure 2b. At last, the final core used was the Gyroid's core using a 15mm edge. A 1.58mm filling was used. The core can be seen in Figure 2c.

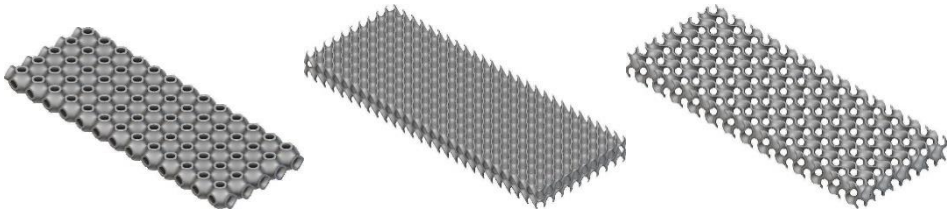

(a) (b) (c)

Figure 2 - Cores with different configurations. (a) TPMS Primitive core TPMS Diamond core (c) TPMS Gyroid core

The faces were modeled according to the circuit boards acquired. Each face has a length of 200mm, a width of 75mm and a thickness of 1.6mm.

5.2 Numerical Analysis

The numerical analysis was done according to the following steps. After modeling the core, the faces were positioned at the superior and inferior edges of the core. A discrete mesh was created to convert the core from an implicit object to a discrete object. Afterwards, the discrete mesh was transformed into a volumetric mesh. At last, the mesh was transformed into a finite element mesh, making it possible to export the mesh as a .cdb format.

After the creation of the .cdb file for the mesh, the file was exported to the *Ansys Workbench* in the *External Model* tab. The *External Model* tab was connected to the *Static Structural* tab in the *Model* section. The properties of the materials were defined in the *Engineering Data* section. The

materials of the core and the faces were modeled as isotropic, according to what was studied by (Wernke, 2019). The properties used for the numerical analysis are shown in table 1.

Table 1 - Material's properties used in the numerical analysis.

Parameter	Young's modulus/ MPa	Poisson's ratio
FR-4(1)	3.42	0.25
PLA(2)	2.85	0.3

Note: (1) Properties obtained according to Madhukar *et al.* [2018]
(2) Properties obtained according to Santana *et al.* [2021]

Lastly, the constraints were defined aiming to be similar to the 3-point bending tests. 2 fixed supports in the lower face and a central line for the application of the force were determined.

Analytical Calculation

In order to acquire data to compare the obtained results from the Finite Element Method with the results obtained experimentally, a stress analysis on the face and on the core was performed according to the standard ASTM C393. No analytical calculation for the deflection was done due to the impossibility of predicting the shear modulus Gc of the core. The equations 4 and 5 were used to determine the shear modulus in the core and the normal stress on the faces.

$$F_s = \frac{P\_max}{(d+c)^b} \quad (4)$$

$$\sigma_s = \frac{P\_max * L}{2t(d+c)^b} \quad (5)$$

Considering *Fs* is the shear modulus of the core, *Pmax* is the maximum load, *d* is the thickness sandwich, *c* is the thickness of the core, *b* is the width, σf is the stress on the face, *L* is the length and *t* is the thickness of the face.

5. 3 Topology Optimization

The Topology Optimization was done using the software, *Ansys Workbench*. The process was initially performed by modeling a solid block using the core's dimensions. Afterwards, the faces were positioned with the same dimensions as the circuit boards used. The core was modeled as a PLA solid block and the faces using the properties of the circuit board's material. The conditions applied were the same as the ones used on the 3 points bending test, using a central load on the upper face and two fixed supports on the lower face distanced by 150mm from each other.

After performing a static analysis of the sandwich structure, the results were exported to the topology optimization tab. The next step was defining the optimization properties. The percentage of mass chosen was 30% similar to the ratio between a honeycomb core and a solid core. The results obtained showed a concentration of mass around the region of the supports.

The next step was the optimization of the TPMS core using the geometry obtained. The distribution of the mass in relation to the length of the core was converted into a matrix and represented by Eq. 6.

$$A_{ixj} = \begin{bmatrix} 0 & 0 \\ 25 & 1 \\ 50 & 0 \\ 100 & 1 \\ 150 & 0 \\ 175 & 1 \\ 200 & 0 \end{bmatrix} \quad (6)$$

Considering A_{ixj} as the matrix, a_{ix1} as the terms that represent the position of the core in relation to the length and a_{ix2} as the terms that indicate the presence or absence of mass.

After getting the matrix, a numerical interpolation using the least squares method in order to obtain a sinusoidal function that fits the distribution. The equation is described in Eq. 7.

$$f(x) = sen^2(2.014 \times 10^{-8}x^4 - 6.717 \times 10^{-4}x^2 + \pi) \quad (7)$$

This distribution of mass was used in the software nTopology to blend the core with the lower mass (represented by 0) and the core with the higher mass (represented by 1). The intermediate regions between 0 and 1 represent the variation of thickness between the two cores designed. Figure 3 shows the distribution of mass obtained. The table 2 below shows the properties of the modeled cores:

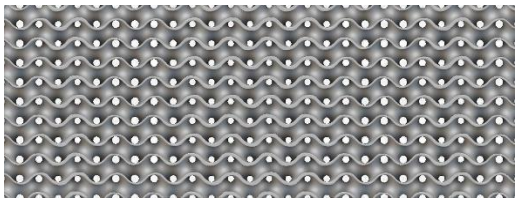

Figure 3 – TPMS Distributed core

Table 2 - Properties of the modelled cores.

Parameter	Honeycomb	Gyroid Base	Gyroid Distributed
Size of the cell (mm)	-	15	15
Minimum thickness (mm)	-	1.58	1
Maximum thickness (mm)	-	1.58	2.02
Volume (mm^3)	48509.2	48509.2	48509.2

5.4 Manufacturing Process

The cores of the TPMS base configuration were manufactured using an FDM 3D printer model 8 from the brand *Anet*. Using a printing area of 300mm in length, 300mm in width, and 400mm in height, the printing parameters used are shown in Table 3.

Table 3- Printing Parameters for the TPMS base core.

Printing Parameters	Value
Diameter of the nozzle	0.4 mm
Temperature of the extruder nozzle 1° layer	205 ºC
Temperature of the extruder nozzle 2° layer	200 ºC
Temperature of the table	65 ºC
Thickness of the layer	0.2 mm
Printing speed	30 m/min
Filling	100 %

For the printing of the cores with distribution of mass, a printer from the brand Creality model Ender 3, was used. The material used was PLA from the brand 3D Lab. Its properties are described in Table 4.

Table 4- Printing Parameters for the TPMS distributed core.

Printing Parameters	Value
Diameter of the nozzle	0.4 mm
Temperature of the extruder nozzle 1° layer	205 ºC
Temperature of the extruder nozzle 2° layer	200 ºC
Temperature of the table	65 ºC
Thickness of the layer	0.8 mm
Printing speed	50 m/min
Filling	100 %

The epoxy resin 2004 and the epoxy resin hardener 3154 were used to produce the samples. The laminated faces were acquired at 200mm in length, 150mm in width, and 1.5mm in thickness. The faces were sliced using a Dremel, and got the dimensions to 200mm in length, 75mm in width, and 1.6mm in thickness. To improve its adherence, the laminated faces were sanded, and the protective film was removed.

The next step was preparing the epoxy resin according to the provider's specifications. A proportion of 100% resin and 50% catalyst was used. Furthermore, the core and faces went through a lamination process. This process consists of fixing the core and faces using epoxy resin. The resin was scattered on the faces and positioned on the laminating bench.

In order to perform the lamination, the samples were submitted to vacuum. According to Sant'Ana and Carvalho (2020), the use of vacuum reduces the number of bubbles and empty spaces in the resin, improving the adherence of the materials. Initially, the laminating bench was prepared by delimiting its space by using Tacky Tape inside the area where a layer of wax worked as a mold release agent. Afterwards, the test specimens were positioned, and above them, a layer of Peel Ply, a layer of perforated film, and a bleeder layer were introduced. A hose connected to a vacuum pump was inserted, and the whole system was covered using a vacuum bag (Sant'Ana *et al.*, 2019). The specimens were submitted to vacuum for a period of 6 hours. The Figure 4a demonstrates how the system was built. The process utilized the same configurations for the TPMS base and the TPMS distributed.

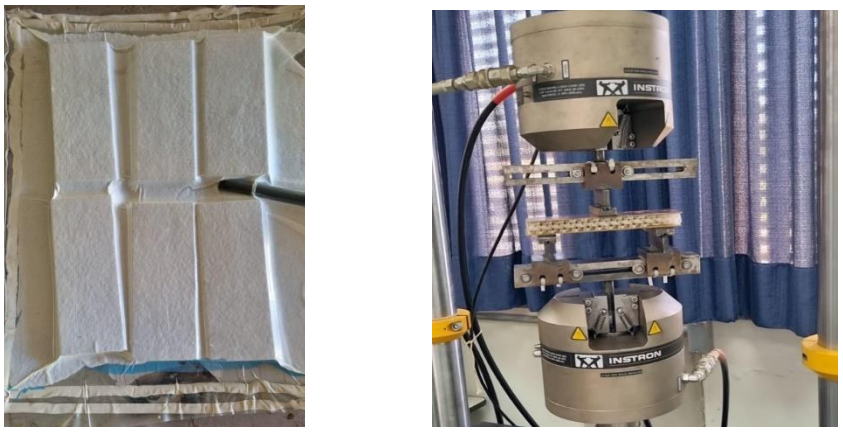

(a) (b)

Figure 2 – Manufacturing and tests. (a) Lamination Bench (b) Three Point Bending Test.

5.5Three Point Bending Test - ASTM C393

To analyze the resistance of the sandwich panels manufactured, a test according to the standard ASTM C393 was performed. The test consists of determining the properties of a flat sandwich after being flexed and producing the curvature of the facing planes of the sandwich (ASTM, 2000). It's possible to determine properties such as the sandwich flexural stiffness, the core shear strength and shear modulus, or the facings compressive and tensile strengths. Six specimens of the TPMS base configuration and six specimens of the TPMS distributed configuration

were submitted to the 3-point destructive test. Therefore, with the data obtained, it was possible to compare the analytical calculations and the numerical analysis performed with the numerical simulation software, as well as the honeycomb sandwich structure manufactured before. The Figure 4b illustrates how the test was performed.

The test was performed using a servo-hydraulic system for a fatigue test, Instron 8801. The velocity of the test was set at 1 mm/min, in a way that the failure occurred between 3 and 6 minutes. The length L between the supports was defined as 150mm, as defined by the standard ASTM C393.

6. Results

The samples of the TPMS base configuration had a mass of 170.2g and a density of 0.591 g/cm^3. While the specimens of the TPMS distributed configuration had a mass of 175.4g/cm^3 and a density of 0.609g/cm^3. Figure 5a shows one of the specimens of the TPMS distributed configuration produced.

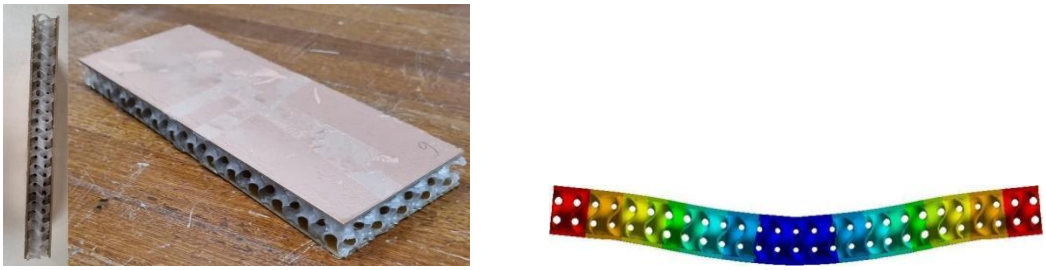

(a) (b)

Figure 5 – Real and simulated sandwich. (a) TPMS Distributed sandwich (b) TPMS Distributed sandwich simulation.

For the purpose of comparing the values obtained for the displacement in the experimental and numerical methods, a force of 1000 N was chosen. The results obtained are shown in Table 5 and indicate a good correlation between the data. The geometry simulated can be seen in Figure 5b. As observed in Table 5, it's possible to verify some percentile error of the numerical analysis in relation to the experimental value obtained.

Table 5 - Comparison between numerical analysis and experimental.

Properties	TPMS Base	TPMS Distributed
Load	1000 N	1000 N
Experimental deflection	0.93297	1.1777
Numerical deflection	0.92233	1.235
Error	1%	5%

After performing the tests, it was possible to obtain a maximum load value of 5966.2 N and a maximum displacement of 5.8404mm for the samples of the base distribution. Furthermore, it was also possible to compare the displacements between the analytical, numerical, and experimental data for the base configuration, as shown in Figure 6a. Meanwhile, for the TPMS distributed configuration, the maximum load achieved was 2061.0 N and a maximum displacement of 3.449mm. It's possible to compare the displacement data in Figure 6b. The values are clustered in Table 6.

Table 6 – Experimental Data.

Properties	TPMS Base	TPMS Distributed
Load	5966.2 N	2061.0 N
Maximum Displacement	5.8404 mm	3.449 mm

In Figure 8, it is possible to compare the force and displacement curves for the Base and Distributed configurations. It can be observed that the TPMS Base resisted a higher load, resulting in a higher displacement. This is probably due to micro-fractures inside the TPMS Distributed's core, because the core failed in the lowest concentrated mass area. It's also noticeable that for loads lower than 1000 N, the curves are very similar due to the faces of both panels being the same.

Therefore, it's possible to compare force, displacement, and density between TPMS Base and TPMS Distributed. After calculating the percentage difference, a 65% difference in the max load and stresses was noticed, while there was a change in density of only 3%. Table 7 shows the comparison of the TPMS core's properties.

Furthermore, the failure modes of the sandwich panels provide important aspects. In both the TPMS Base and the TPMS Distributed that were tested, a fracture inside the core was noticed, described by Bitzer (1997) as transversal shear failure. This failure occurs due to insufficient resistance to shear inside the core. The Figures 7a and 7b show the fracture of the sandwich panels.

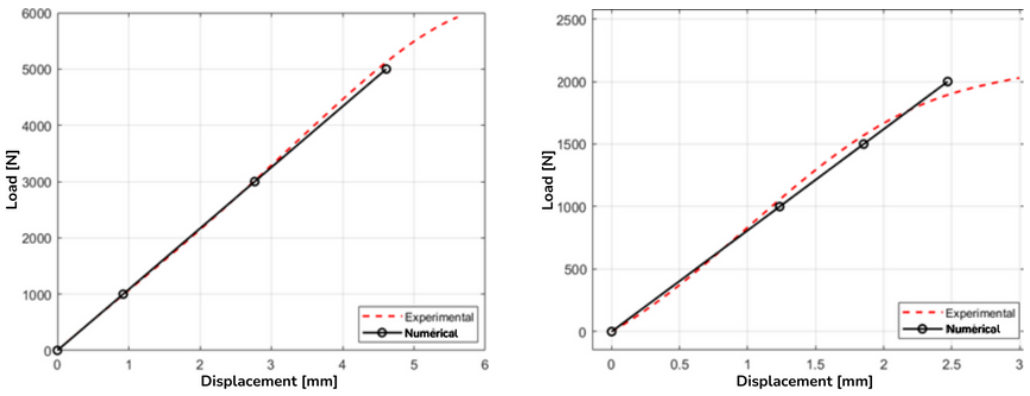

(a) (b)

Figure 6 - Load X Deflection curves. (a) TPMS Base core (b) TPMS Distributed core

Table 7 - Percentage difference between the properties.

Parameter	TPMS Base	TPMS Distributed	Percentage
Maximum load [N]	5966.2	2061.0	-65%
Maximum deflection [mm]	5.8404	3.449	-41%
Density [g/cm3]	0.591	0.609	3%
Stress on face [MPa]	2.2599	0.7807	-65%
Stress on core [MPa]	141.24	48.79	-65%

(a) (b)

Figure 7 - Fracture tests. (a) TPMS Base sandwich (b) TPMS Distributed sandwich

According to Petras (1998), it's possible to predict failure modes as well as analyze the failure modes agents. For this study, there weren't any failures due to the manufacturing process, such as the delamination of faces observed by Carvalho (2019) in his aluminum samples. All of the failures presented fragile behavior, meaning there was no hardening zone. The fragile behavior was expected, as shown in the studies performed by Ribeiro (2019) and Santana et al. (2018).
We can also compare the data obtained with the TPMS core and the data from previous works using the Honeycomb core. The Figure 8 shows the relationship between force and displacement between the three configurations. The table 8 shows the values obtained through the experiments.

Table 8 - Relation to the Honeycomb sandwich.

Properties	Honeycomb	TPMS Base	TPMS Distributed
Maximum load [N]	8086.6	5966.2	2061.0
Maximum deflection [mm]	6.1481	5.8404	3.449
Density [g/cm3]	0.692	0.591	0.609
Stress on face [MPa]	3.06	2.2599	0.7807
Stress on core [MPa]	143.58	141.24	48.79

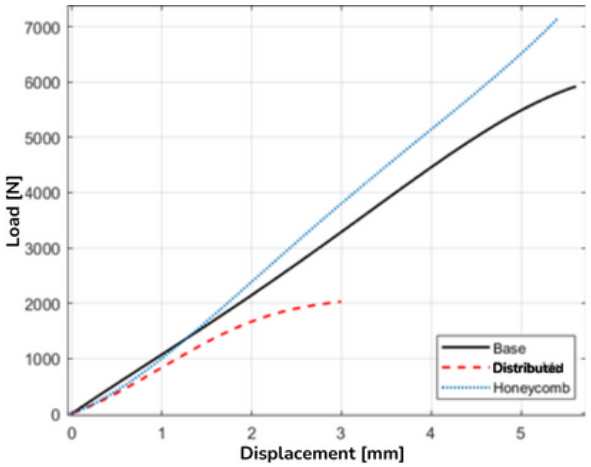

Figure 8 – Comparison between the TPMS Base, TPMS Distributed and Honeycomb configurations.

7. Conclusions

It is possible to observe that the results obtained through the Finite Element Method in relation to the experimental method indicate an excellent correlation. Despite the core of the TPMS Distributed configuration not presenting any visible improvement, it was possible to perceive that although it presented a fragile fracture with a lower load, it wasn't catastrophic. For the purpose of this work, the TPMS Base structure demonstrated great mechanical properties and although its properties were inferior to the honeycomb structure it has a lower mass. Furthermore, the TPMS presented great energy absorption, making it possible to be applied to studies involving impacts. In future studies, it is suggested to perform the impact analysis of the cores and to produce and characterize cores with flexible filaments, such as TPU. Depending on the results obtained, different applications can be explored for these types of structures, especially for aerospace appliance. Therefore, considering the focus of this work, the sandwich panels constructed can be applied to Cubesat and be submitted to other tests, such as random vibrations test (represent the vibrations occurred during the launching of the vehicle), essential for the validation of the satellite structure.

References

ASTM International. (2000). *Standard Test Method for flexural properties of sandwich constructions. In American Society for Testing and Materials Annual Book of ASTM Standards* (Vol. 30, p. 32). West Conshohocken, PA, USA.

Bitzer, T. (1997). *Honeycomb core. In T. Bitzer (Ed.), Honeycomb Technology: Materials, Design, Manufacturing, Applications and Testing* (pp. 10-42). Dordrecht: Springer Netherlands.

Carvalho, L. R. (2019). *Fabricação e caracterização de estruturas sanduíche tipo colmeia com núcleo impresso por fusão e deposição de material termoplástico*. Trabalho de Conclusão de Curso, UnB (Universidade de Brasília), Brasília, Brasil.

Decker, L. H., & Frantz, J. C. (2022). *Análise compressiva do preenchimento giroide em peças fabricadas por fdm*. Revista da UNIFEBE, 27, 476 498.

Gagliardo, D. P., & Mascia, N. T. (2010). *Análise de estruturas sanduíche: Parâmetros de projeto. Ambiente Construido*, 10, 247 258.

Gibson, I, Rosen, D, & Stucker, B. (2015). *Additive manufacturing technologies 3d printing, rapid prototyping, and direct digital manufacturing*. Springer.

Han, L., & Che, S. (2018). *An overview of materials with triply periodic minimal surfaces and related geometry: From biological structures to self-assembled systems*. Advanced Materials, 30, 22.

Henrique Júnior, S. S., Moura, F. P., Correa, R. S., Afonso, J. C., Vianna, C. A., & Mantovano, J. L. (2013). *Processamento de placas de circuito impresso de equipamentos eletroeletrônicos de pequeno porte*. Química Nova, 36, 570 576.

Hermann, K., & Konrad, P. (1996). *Construction of triply periodic minimal surfaces*. Phil. Trans. R. Soc. A., 354, 2077 2104.

Hsieh, M.-T., & Valdevit, L. (2020). *Minisurf a minimal surface generator for finite element modeling and additive manufacturing*. Software Impacts, 6, 5.

LaDou, J. (2005). *Printed circuit board industry*. International Journal of Hygiene and Environmental Health, 209, 211 219.

Logan, D. L. (2011). *A first course in the finite element method*. Thomson.

Madhukar, D. K., Dutta, S. R., Mahto, P. K., Sinha, A. K., & Das, P. P. (2018). *Random spectral analysis of integrated avionics module*. IOP Conference Series: Materials Science and Engineering, 377.

Moaveni, S. (2007). *Finite element analysis: Theory and application with ansys*. Pearson.

Petras, A. (1998). *Design of sandwich structures* . Doctoral dissertation, Cambridge University, Engineering Department.

Ribeiro, G. P. (2019). *Caracterização mecânica de estruturas manufaturadas por adição de material termoplástico com diferentes níveis e formas de preenchimento*.

Sant'Ana, M. S., Alves, P. H. S., Santos, T. R., & Jr., M. N. D. B. *Análise numérica e experimental de painéis sanduíche fabricados com núcleo termoplástico e faces laminadas*. In Cobef congresso brasileiro de engenharia de fabricação. Curitiba, Brasil, 2021.

Sant'Ana, M. S., Gomes, M. L. C., & Jr, M. N. D. B. *Analysis of the influence of the cure and post-cure processes on fiberglass composites*. In Cobem. Curitiba, Brasil, 2019.

Santana, L, Alves, J. L., Netto, A. C. S., & Merlini, C. (2018). *Estudo comparativo entre PETG e PLA para impressão 3D através de caracterização térmica, química e mecânica*. Revista Matéria, 23.

Schwingel, D., et al. (2007). *Aluminium foam sandwich structures for space applications*. In 57th International Astronautical Congress (p. C2.4.10).

Tran, P., & Peng, C. (2021). *Triply periodic minimal surfaces sandwich structures subjected to shock impact*. Journal of Sandwich Structures & Materials, 23, 2145 2175.

Vyavahare, S., Teraiya, S., Panghal, D., & Kumar, S. (2020). *Fused deposition modelling: A review*. Rapid Prototyping Journal 26, 176 201.

Wernke, A. P. (2019). *Caracterização e avaliação da preditibilidade de modelos isotrópicos e ortotrópicos para materiais impressos com foco em otimizações topológicas* (Term Paper, UnB (Universidade de Brasília), Brasília, Brasil).

Zhang, W., Zhu, J., & Gao, T. (2015). *Topology optimization in engineering structure design*. Elsevier.

Zhu, Ji-Hong, Zhang, Wei-Hong, & Xia, Liang. (2016). *Topology optimization in aircraft and structures design*. Archives of Computational Methods in Engineering, 23, 595-622.

Zou, R, Xia, Y, Liu, S, Hu, P, Hou, W, Hu, Q, & Shan, C. (2015). *Isotropic and anisotropic elasticity and yielding of 3d printed material*. Composites Part B, 99, 505 513.